

**Design of a heterostructure peapod using magic silicon clusters**Q. Sun,<sup>1,2</sup> Q. Wang,<sup>1,2</sup> Y. Kawazoe,<sup>1</sup> and P. Jena<sup>2</sup><sup>1</sup>*Institute for Materials Research, Tohoku University, Sendai 980-77, Japan*<sup>2</sup>*Physics Department, Virginia Commonwealth University, Richmond, Virginia 23284*

(Received 19 July 2002; published 31 December 2002)

We show that the fabrication of one-dimensional Si nanostructures with tailored electronic structure and optical properties can be achieved by encapsulating magic metal-doped Si clusters in carbon nanotubes. This cannot only effectively change the properties of the so-called peapod, but also can keep the intrinsic structure of Si clusters growing in one dimension due to its confinement by the nanotube. Using density functional calculations, the minimum tube size is found to be (9,9) for encapsulating magic WSi<sub>12</sub> clusters. Due to its nonspherical shape, the interaction of the magic cluster with the tube is orientation dependent. The larger atomic size of Si also forces the cluster-tube and cluster-cluster distances to be larger than those of a C<sub>60</sub>@C tube, resulting in a weaker interaction with the tube. The experimental optical absorption spectra are well reproduced for empty carbon nanotubes, which can be greatly changed with WSi<sub>12</sub> encapsulation, thus enabling the nanoheteropeapod to have important applications in nanodevices.

DOI: 10.1103/PhysRevB.66.245425

PACS number(s): 61.46.+w, 71.20.Tx, 61.48.+c, 36.40.Cg

**I. INTRODUCTION**

Small atomic clusters containing about a dozen atoms constitute subnanoscale systems that exhibit unique size and composition specific properties. It has been suggested<sup>1</sup> that assembling these clusters into bulk form, while maintaining their structural integrity, can lead to a novel route for the synthesis of cluster assembled materials with tailored properties. Since the atomic clusters are in general metastable, they tend to coalesce when brought into each other's vicinity. To minimize or prevent the possibility of this coalescence it is necessary either to start with clusters that are unusually stable (so-called magic clusters) and/or isolate them in matrices. Recent discoveries of carbon fullerenes<sup>2</sup> and nanotubes<sup>3</sup> have provided a way in which clusters can be assembled. The C<sub>60</sub> carbon fullerenes are so stable that they can be assembled without passivation to form a bulk crystal. These fullerenes containing endo- or exohedral metal atoms can also be assembled to form bulk structure. Individual single-wall carbon nanotubes (SWNT's), on the other hand, enclose a cylindrical empty space which can be filled with atoms or clusters. One such system consists of C<sub>60</sub> clusters embedded inside a nanotube and resembles the structure of a peapod. We call this as homopeapod as both fullerenes and nanotubes consist of carbon atoms. The first homopeapod C<sub>60</sub>@SWNT's was observed in material prepared by laser ablation using high-resolution transmission electron microscopy (TEM).<sup>4</sup> Thus studies of peapods link the cluster science and nanotube science. The excitement in the research of nanopeapods arises from the fact that one can vary the size and composition of the embedded clusters as well as the size of the nanotube, thus providing flexibility in their synthesis.<sup>5-11</sup> Recent measurements of the electronic and structural properties for the homonapeapods have been performed using electron-energy-loss spectroscopy in transmission mode.<sup>12</sup> It has been found that C<sub>60</sub> peapods with a SWNT diameter distribution of 1.29–1.45 nm have an average fullerene filling of 60%. However, as for the electronic and optical properties, the overall shape of the response of

the SWNT and the peapods is very similar: the difference exists only in the fine structure. This indicates that there are no big changes in the properties of the homopeapod of a C<sub>60</sub>@C tube compared to the empty C tube. This experiment proposed a new challenge for the studies of the peapod. Can one find a suitable cluster that, when inserted into the nanotube, will change the properties of the nanotube?

In this paper, we investigate the design of a heteropeapod in which non-carbon-based clusters are inserted into a carbon nanotube. In order to form such a peapod, the encapsulating clusters should be stable by themselves to reduce the possibility of their coalescence. We have chosen the WSi<sub>12</sub> cluster as dopant due to the following reasons: Silicon plays an integral part in electronic devices. Although Si is tetravalent like C, Si clusters do not form cagelike structures. In a recent experiment, WSi<sub>12</sub> has been found to be a magic cluster.<sup>13</sup> Theoretical studies show that it is composed of two hexagonal rings with a W atom in its center. This new magic cluster has attracted wide publicity and interest because of the possible applications of silicon cage clusters in nanoscience and nanoelectronic devices.<sup>14-17</sup> One very basic question is how to assemble this much promising magic cluster? It is natural to imagine the possibility of constructing a one-dimensional chain of these caged clusters. However, detailed studies<sup>18</sup> of their dimer indicate that in free space the two clusters interact and consequently their structures are seriously destroyed. Thus it is difficult to construct a one-dimensional Si nanostructure in free space using this WSi<sub>12</sub> tube-shaped unit. We discuss an alternate possibility where the magic WSi<sub>12</sub> cluster is inserted into a C nanotube. There are several questions that need to be addressed. (1) What is the minimum tube size to encapsulate this magic cluster? (2) What is the favorable orientation of this nonspherical cluster in the carbon tube? (3) How strong are the interactions between the cluster and tube? (4) How far apart should the two Si clusters be in the tube? (5) Are the properties of this heteropeapod different from that of the empty tube and/or the homopeapod of the C<sub>60</sub>@C tube? In the following we describe our theoretical procedure and results.

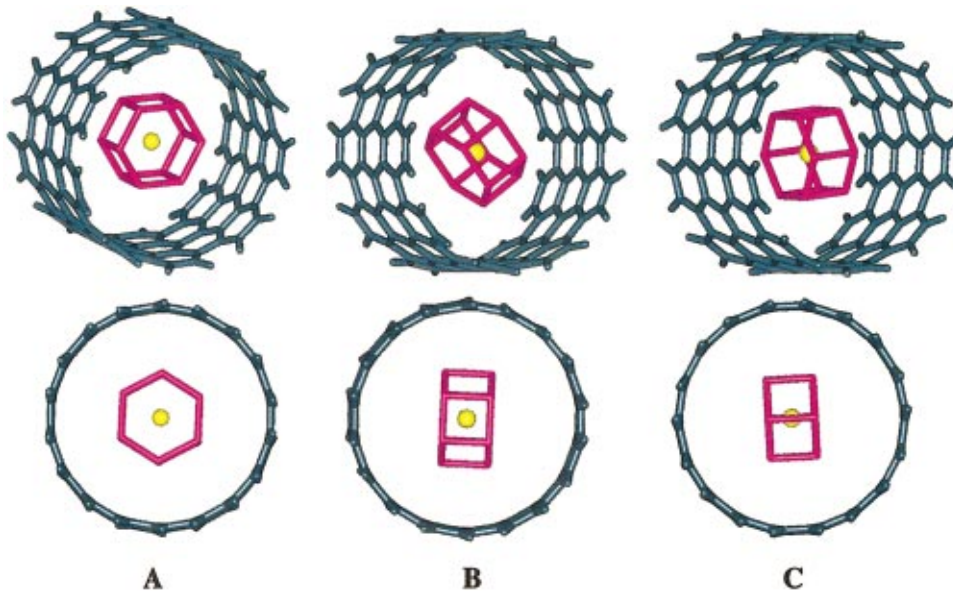


FIG. 1. (Color) Three orientations of the magic  $WSi_{12}$  cluster inside the carbon nanotube.

## II. COMPUTATIONAL PROCEDURE

We have performed *ab initio* calculations using an iterative solution of the Kohn-Sham equations, based on the minimization of the norm of the residual vector to each eigenstate and an efficient charge density mixing.<sup>19,20</sup> For the exchange-correlation functional, gradient-corrected functionals in the form of the generalized gradient approximation<sup>21</sup> (GGA) have been chosen. In order to optimize geometry effectively, a plane-wave basis set is adopted with the projector-augmented-wave (PAW) method originally developed by Blöchl<sup>22</sup> and recently adapted by Kresse and Joubert.<sup>23</sup> The particular advantage of the PAW method over the ultrasoft pseudopotentials is that the pseudization of the augmentation charge can be avoided. The structure optimization is symmetry unrestricted and carried out using conjugate-gradient algorithm. Since experimentally it is not yet possible to synthesize a perfect nanotube of “infinite” length, we have considered a tube with finite length. The dangling bonds are terminated with H atoms, which does not produce any localized states near the tube edges.<sup>24</sup> We used supercells with 12-Å vacuum spaces along  $x$ ,  $y$ , and  $z$  directions for all the calculated peapods. The Gamma point is used to represent the Brillouin zone due to the large super-

cell. The cutoff energy is 300 eV, and the convergence criteria for energy and force are  $10^{-4}$  eV and 0.002 eV/Å, respectively.

In the present calculations, we used armchair tubes as they are energetically more stable.<sup>25</sup> To reduce the computa-

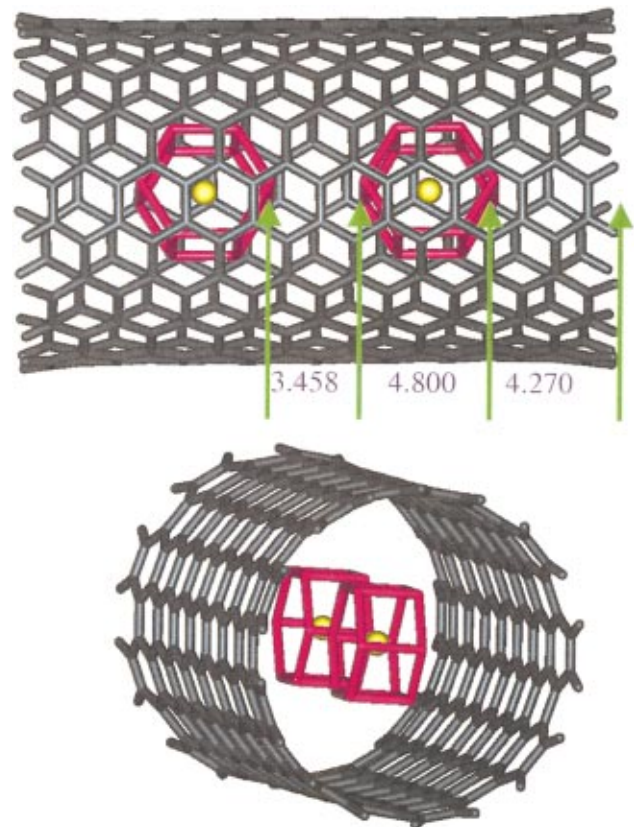


FIG. 3. (Color) Preferable orientation of the cluster dimer inside the carbon nanotube of (9, 9). The bonds between Si atoms and W atoms are not shown for the sake of simplicity. The distances between the clusters and the cluster and tube edge as well cluster sizes are also shown.

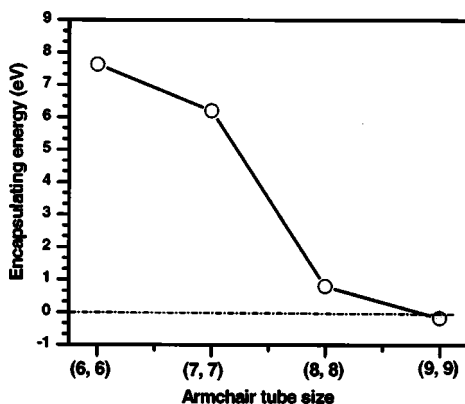


FIG. 2. Encapsulation energy changes with nanotube size.

tional costs, the supercells are chosen with different sizes for different purposes. To determine the minimum tube size for encapsulating this magic cluster, (6, 6), (7, 7), (8, 8), and (9, 9) tubes with 9.22 Å length are used, which are composed of (84C, 24H), (98C, 28H), (112C, 32H), and (126C, 36H) atoms, respectively. The  $\text{WSi}_{12}$  cluster is put in the central part of the tubes. Due to the nonspherical shape of  $\text{WSi}_{12}$ , the interactions are orientation dependent, which makes the calculations more costly as compared with the  $\text{C}_{60}$  case. We have chosen three typical orientations as shown in Fig. 1: (1) sixfold axis of the cluster aligned parallel to the tube axis (configuration A), (2) twofold axis (through the two opposite squares) of the cluster aligned parallel to the tube axis (configuration B), and (3) twofold axis (through the two opposite edges) of the cluster aligned parallel to the tube axis (configuration C).

The encapsulating energies are defined as the energy cost in inserting a  $\text{WSi}_{12}$  cluster into the nanotube: namely,

$$DE = E[\text{WSi}_{12}@\text{tube}] - E[\text{tube}] - E[\text{WSi}_{12}]. \quad (1)$$

### III. RESULTS AND DISCUSSION

The encapsulating energies in Eq. (1) are shown in Fig. 2 for the four tube sizes. Due to the small size of (6, 6), (7, 7), and (8, 8), the  $\text{WSi}_{12}$  cluster is seriously distorted and unfavorable energetically. The (9, 9) tube is the smallest one for encapsulating this magic cluster. The encapsulating energies for the (9,9) tube are  $-0.071$ ,  $-0.133$ , and  $-0.176$  eV for the configurations of A, B, and C, respectively. Therefore, the favorable orientation is configuration C. The shortest distance  $D$  between the cluster and the tube wall is 4.138 Å. This can be understood using the following simple argument: It has been found that the smallest tube to encapsulate  $\text{C}_{60}$  is (10,10), and the shortest distance  $D_0$  between  $\text{C}_{60}$  and the tube wall is 3.31 Å.<sup>6</sup> This distance can be approximated by using the sum of atomic radii  $R$  with some scale factor  $K$ . In the  $\text{C}_{60}@\text{C}$  tube case,  $D_0 = K(R_C + R_C)$ , while in the Si case,  $D = K(R_{\text{Si}} + R_C)$ . (Because Si and C have the same valence configurations, the scaling factor  $K$  can be taken to be the same value in the first order approximation.) We know that the Si atom is 1.5 times larger in radius than the C atom, so  $D = 2.5 \times K \times R_C$ . This yields  $D/D_0 = 1.25$ , which is exactly the ratio of cluster-tube distances between  $\text{WSi}_{12}$ - and  $\text{C}_{60}$ -doped systems (4.138 to 3.31). The larger distance in the  $\text{WSi}_{12}$  case results in weaker interactions with the tube as compared with the  $\text{C}_{60}$  case, where the encapsulating energy is  $-0.51$  eV.<sup>6</sup> Therefore, we can see that size is a main factor to determine whether a cluster can be encapsulated or not.

We have next examined the case where two  $\text{WSi}_{12}$  clusters are inserted into the nanotube. For this purpose, we used the (9,9) tube with length of 21.6 Å, which contains 306 C atoms and 36 H atoms. Two clusters are put symmetrically in the tube with orientation C (Fig. 1), and the initial distance is set to be 2.3 Å (the bond length in bulk Si). The structure of the dimer after full optimization is shown in Fig. 3. The equilibrium distance between the two clusters became 3.458 Å, which is larger than 3.14 Å in the  $\text{C}_{60}$  case.<sup>6</sup> Note that with this distance between the clusters, each  $\text{WSi}_{12}$  is 4.27 Å

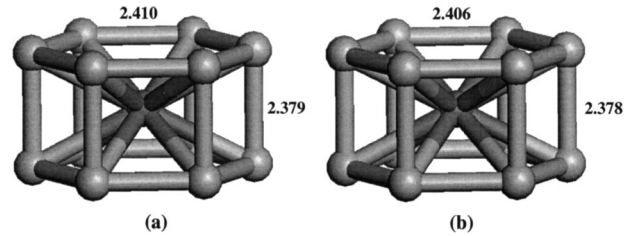


FIG. 4. Geometrical structure of  $\text{WSi}_{12}$  with  $D_{6h}$  symmetry in free space (a) and in the nanotube (b).

from the edge of the tube. This is significantly larger than the dimer bond length, and thus we do not expect properties of the embedded dimer to be affected by edge effects. The structure of the embedded  $\text{WSi}_{12}$  cluster remains essentially unaltered from that of its gas phase structure. This can be clearly seen from Fig. 4, where we have compared these two structures in free space and in the carbon nanotube. The bond length changes only a little bit, and the  $D_{6h}$  symmetry also remains unchanged. This results from a weak interaction between the clusters and between the clusters and tube. This can be demonstrated by examining the charge density profile plotted in Fig. 5. In Fig. 5(a) we have shown the charge density contours corresponding to densities in the range of  $0.1$ – $1.0 e/\text{Å}^3$  along the dimer axis, while that in Fig. 5(b), it corresponds to charge distributions in the plane perpendicular to the dimer axis. We can see that there is very little overlap in density between the clusters or between the cluster and tube wall.

It is very interesting to note that due to the confinement of the tube wall, the two clusters can only move along the tube axis, and the intrinsic structure of the cluster itself can be kept. In this way one-dimensional Si nanostructures can be fabricated, which is totally different from the situations in free space.<sup>18</sup> This can be understood as follows: The larger number of core electrons in Si makes it much more difficult for two Si atoms to form double or triple bonds. Conse-

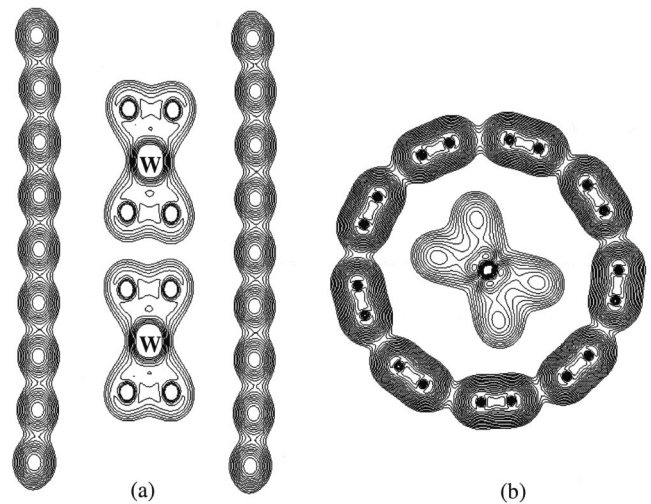


FIG. 5. Charge density contour plots on the planes through the tube axis (a) and perpendicular to the tube axis (b) in the range of  $0.1$ – $1.0 e/\text{Å}^3$  with contour spacing  $0.05 e/\text{Å}^3$ .

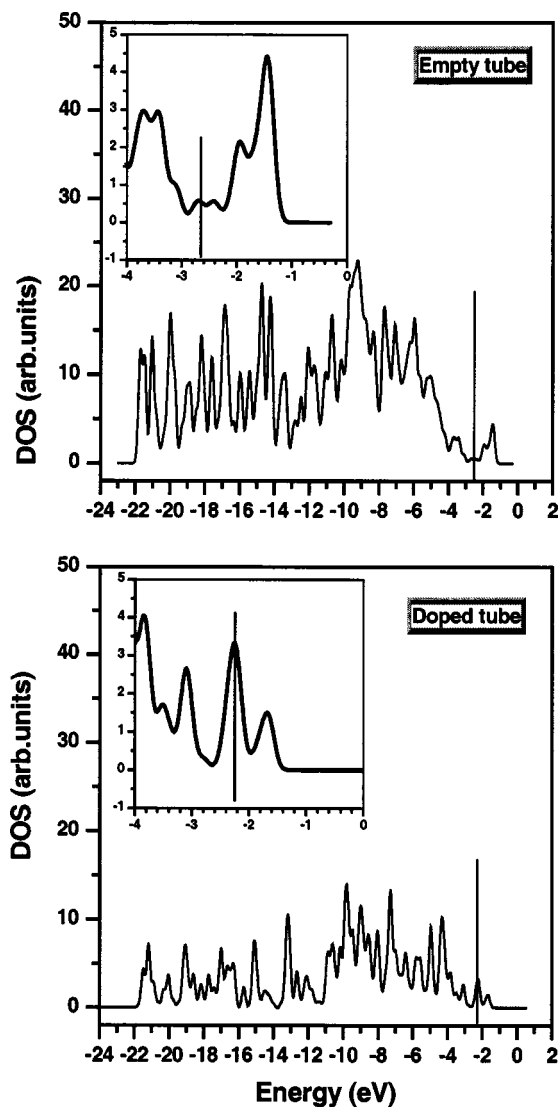


FIG. 6. DOS for the empty tube (a) and for the peapod (b): smaller energy windows are given around the Fermi level.

quently, Si prefers to form multidirectional single bonds ( $sp^3$ ). Since there are no constraints in free space, clusters often aggregate and the composite structure is rebuilt due to the new bonding requirement.

We now examine if the electronic structure and properties of the heteropeapod are different from those of the homopeapod or empty tube. In Fig. 6, we compare the electron density of states (DOS) between the empty tube and heteropeapod. In order to see clearly the changes of the DOS near the Fermi level, smaller energy windows are also shown. The DOS at the Fermi energy of the empty tube shown in Fig. 6(a) is small, but not zero: this is because the armchair tube is metallic, and the DOS of a finite tube with length of only a few nanometers resembles that of infinite long tubes.<sup>26</sup> The DOS at the Fermi level in the peapod is much higher than that in the empty tube, making the peapod more metallic. This is similar to the impurity states which can be introduced into the gap region when impurities are doped. In order to check the changes in the optical absorption spectrum, further calculations are performed with the DMOL package.<sup>27</sup> Double

numerical atomic basis sets augmented with polarization functions (DNP) are used. The exchange correlation is treated using the generalized gradient approximation prescribed by Perdew and Wang and Becke (BPW91). The calculation for optical absorption spectrum is based on two basic approximations:<sup>27</sup> (1) The absorption is approximated by the dipole transition, and (2) the excited state is described by the Kohn-Sham orbitals of the ground state, which ignores both relaxation effects and more fundamental problems describing excited states within density functional theory (DFT).

For the empty tube, it has been found recently<sup>12</sup> that there are three main absorption peaks at 0.7, 1.3, and 1.8 eV, and the intensity order follows as first peak > third peak > second peak, as shown in Fig. 7(c). These features are well reproduced in our calculations as shown in Fig. 7(a), where the Gaussian expansion with width of 0.1 eV is used. Three peaks are calculated to be at 0.7, 1.2, and 1.7 eV, and the intensity order is also in agreement with experiment.<sup>13</sup> This is particularly gratifying since density functional theory even with the GGA does not yield the band gap in quantitative agreement with experiment. One possible reason is that the approximated method used in the DMOL package for the optical absorption may compensate in some way for the deficiency in DFT. We also note that the small differences between the calculated spectra and the experiment could be attributed to the tube size: we used a (9,9) tube with 12.2 Å diameter, while in experiment the tube size ranges from 12.9 to 14.5 Å.<sup>12</sup> It is very encouraging to see that when  $WSi_{12}$  is encapsulated, the optical absorptions are changed a lot, the peaks are shifted towards the higher energies (1.0, 1.6, and 2.1 eV), and the intensities are also changed, as indicated in Fig. 7(b). This is due to the different geometry and different bonding features in  $WSi_{12}$  and  $C_{60}$ . Therefore, the heteropeapod  $WSi_{12}@C$  tube shows quite different electronic and optical properties as compared to those of the homopeapod  $C_{60}@C$  tube.

#### IV. SUMMARY

In this paper, we have studied the structure, stability, electronic, and optical properties of  $WSi_{12}$  clusters encapsulated in carbon nanotubes. Both Si clusters and carbon nanotubes individually are important subjects in chemistry, physics, and nanomaterial science. We have combined these two technologically important systems into one by designing a heteropeapod. This combination provides more variables for nanomaterials design and control, especially since the tube size as well as the composition of encapsulated cluster can be tuned. Such flexibility could allow one to search for some new nanostructure with exotic properties. Following is a summary of our results: (1) The (9, 9) SWNT is the smallest tube for encapsulating the  $WSi_{12}$  cluster. (2) Of the three configurations of the cluster with respect to the tube considered, the energetically favorable structure is configuration C in Fig. 1, in which the twofold axis through the two opposite edges of the  $WSi_{12}$  cluster is parallel to the axis of the carbon nanotube. (3) The equilibrium distance between  $WSi_{12}$  clusters in configuration C of the (9, 9) tube is 3.46 Å, and the

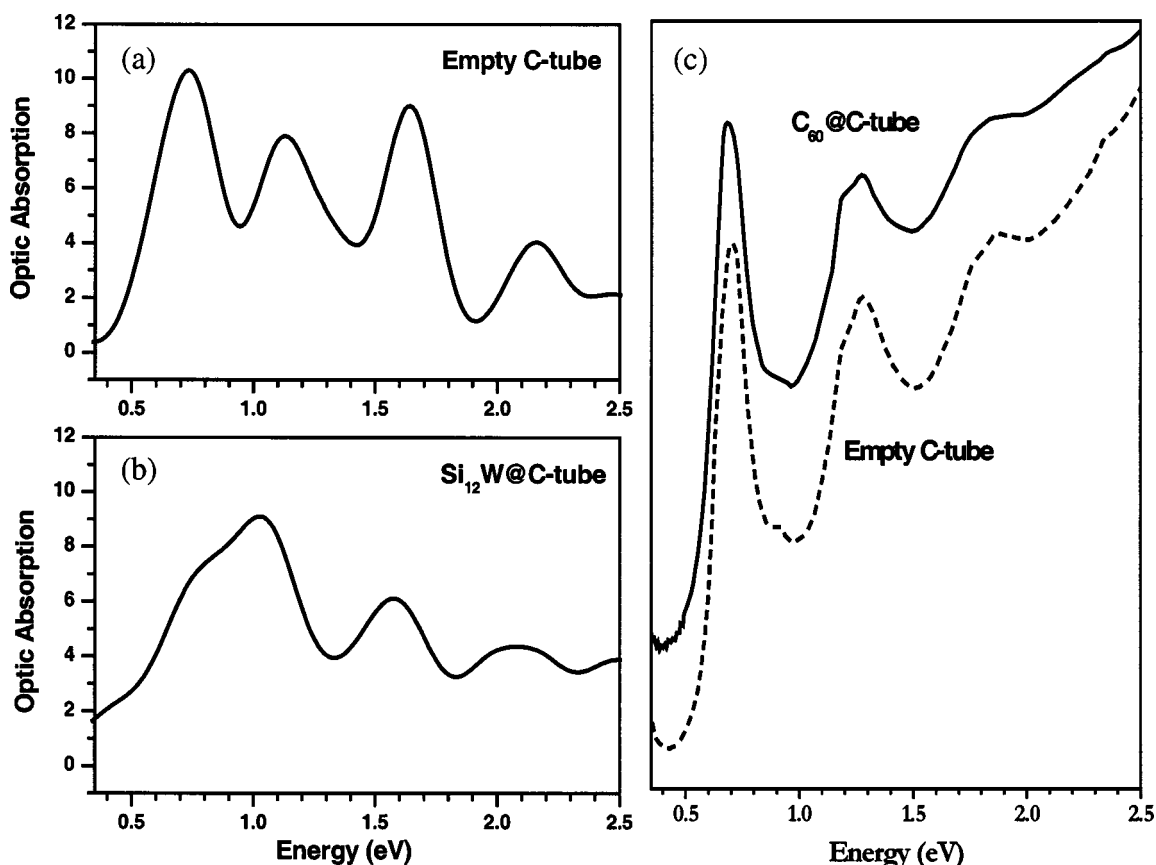


FIG. 7. Optical absorption spectra: (a) Calculated spectra for the empty carbon tube, (b) calculated spectra for the heterostructure of  $\text{WSi}_{12}@C$  tube, and (c) experimental optical absorption spectra for the empty nanocarbon tube and for the heterostructure of  $C_{60}@C$  tube (Ref. 12). The absorption intensity is in arbitrary units.

cluster-cluster and cluster-tube interactions are weak. (4) The electronic density of states at the Fermi energy of this heterostructure is much higher than the empty carbon tube, suggesting that this heterostructure behaves more metallic. (5) The three main absorption peaks in the optical spectrum for the empty carbon nanotube are well reproduced in our calculations, while these absorption peaks are shifted to higher energies and the intensities are changed when  $\text{WSi}_{12}$  clusters are encapsulated. Since the synthesis of  $\text{WSi}_{12}$  cluster,<sup>13</sup> many other metal-stabilized Si cage clusters have been found recently, such as  $M@Si_{16}$  ( $M = \text{Hf}$  and  $\text{Zr}$ ),<sup>28</sup>  $M@Si_{20}$  ( $M = \text{Ba}$ ,  $\text{Sr}$ ,  $\text{Ca}$ ,  $\text{Zr}$ , and  $\text{Pb}$ ),<sup>29</sup> and  $\text{Cr}@Si_{12}$ .<sup>30</sup> It will be inter-

esting to see if these clusters can be assembled inside a carbon nanotube without compromising the structural integrity of the cluster and/or the tube.

#### ACKNOWLEDGMENTS

The authors would like to express their sincere thanks to the crew of the Center for Computational Materials Science, the Institute for Materials Research, Tohoku University, for their continuous support of the HITAC SR8000 supercomputing facility. P.J. would like to acknowledge financial support from the U.S. Department of Energy.

<sup>1</sup>S. N. Khanna and P. Jena, Phys. Rev. Lett. **69**, 1664 (1992); Phys. Rev. B **51**, 13 705 (1995).

<sup>2</sup>H. W. Kroto, J. R. Heath, S. C. O'Brien, R. F. Curl, and R. E. Smalley, Nature (London) **318**, 162 (1985).

<sup>3</sup>S. Iijima, Nature (London) **354**, 56 (1991).

<sup>4</sup>B. W. Smith, M. Monthieux, and D. E. Luzzi, Nature (London) **396**, 323 (1998).

<sup>5</sup>S. Berber, Y. K. Kwon, and D. Tomaneck, Phys. Rev. Lett. **88**, 185502 (2002).

<sup>6</sup>S. Okada, S. Saito, and A. Oshiyama, Phys. Rev. Lett. **86**, 3835 (2001).

<sup>7</sup>B. Bouteaux, A. Claye, B. W. Smith, M. Monthieux, D. E. Luzzi, and J. E. Fischer, Chem. Phys. Lett. **310**, 21 (1999).

<sup>8</sup>B. W. Smith, M. Monthieux, and D. E. Luzzi, Chem. Phys. Lett. **315**, 31 (1999).

<sup>9</sup>J. Sloan, R. E. Dunin-Borkowski, J. L. Hutchison, K. S. Coleman, V. C. Williams, J. B. Claridge, A. P. E. Yorke, C. Xua, S. R. Bailey, G. Brown, S. Friedrichs, and M. L. H. Green, Chem. Phys. Lett. **316**, 191 (2000).

<sup>10</sup>K. Hirahara, K. Suenaga, S. Bandow, H. Kato, T. Okazaki, H. Shinohara, and S. Iijima, Phys. Rev. Lett. **85**, 5384 (2000).

<sup>11</sup>T. Pichler, H. Kuzmany, H. Kataura, and Y. Achiba, Phys. Rev.

- Lett. **87**, 267401 (2001).
- <sup>12</sup>X. Liu, T. Pichler, M. Knupfer, M. S. Golden, J. Fink, H. Kataura, Y. Achiba, K. Hirahara, and S. Iijima, Phys. Rev. B **65**, 045419 (2002).
- <sup>13</sup>H. Hiura, T. Miyazaki, and T. Kanayama, Phys. Rev. Lett. **86**, 1733 (2001).
- <sup>14</sup>Scientific American: News In Brief: Silicon Buckyballs, <http://www.sciam.com/news/022701/1.html>
- <sup>15</sup>Physics News: Silicon Cage Clusters: Better Than Buckyballs? <http://www.aip.org/physnews/update/527-1.html>
- <sup>16</sup>Daily University Science News: Will Silicon Cage Clusters Become The New Buckyballs? <http://unisci.com/stories/20011/0228013.htm>
- <sup>17</sup>Slashdot web site: Silicon Buckyballs=Quantum Bits? <http://slashdot.org>
- <sup>18</sup>Q. Sun, Q. Wang, T. M. Briere, and Y. Kawazoe, J. Phys. C **14**, 33 175 (2002).
- <sup>19</sup>G. Kresse and J. Hafner, Phys. Rev. B **48**, 13 115 (1993).
- <sup>20</sup>G. Kresse and J. Furthmüller, J. Comput. Mater. Sci. **6**, 15 (1996).
- <sup>21</sup>J. P. Perdew, J. A. Chevary, S. H. Vosko, K. A. Jackson, M. R. Pedersen, D. J. Singh, and C. Fiolhais, Phys. Rev. B **46**, 6671 (1992).
- <sup>22</sup>P. Blöchl, Phys. Rev. B **50**, 17 953 (1994).
- <sup>23</sup>G. Kresse and D. Joubert, Phys. Rev. B **59**, 1758 (1999).
- <sup>24</sup>S. Han and J. Ihm, Phys. Rev. B **61**, 9986 (2000).
- <sup>25</sup>D. Sanchez-Portal, E. Artacho, J. M. Soler, A. Rubio, and P. Ordon, Phys. Rev. B **59**, 1758 (1999).
- <sup>26</sup>R. A. Jishi, J. Bragin, and L. Lou, Phys. Rev. B **59**, 9862 (1999).
- <sup>27</sup>Molecular Simulations Ins., computer code DMOL3, version 4.2.
- <sup>28</sup>V. Kumar and Y. Kawazoe, Phys. Rev. Lett. **87**, 045503 (2001).
- <sup>29</sup>Q. Sun, Q. Wang, T. M. Briere, V. Kumar, Y. Kawazoe, and P. Jena, Phys. Rev. B **65**, 235417 (2002).
- <sup>30</sup>S. N. Khanna, B. K. Rao, and P. Jena, Phys. Rev. Lett. **89**, 016803 (2002).